ENERGY-STABLE BACKWARD DIFFERENTIATION FORMULA TYPE FOURIER COLLOCATION SPECTRAL SCHEMES FOR THE CAHN-HILLIARD EQUATION

by

Jun ZHOU[a] and Ke-Long CHENG[b*]

[a] School of Mathematics and Statistics, Yangtze Normal University, Chongqing, China
[b] School of Science, Southwest University of Science and Technology, Mianyang, China

Original scientific paper
https://doi.org/10.2298/TSCI2202095Z

We present a variant of second order accurate in time backward differentiation formula schemes for the Cahn-Hilliard equation, with a Fourier collocation spectral approximation in space. A three-point stencil is applied in the temporal discretization, and the concave term diffusion term is treated explicitly. An additional Douglas-Dupont regularization term is introduced, which ensures the energy stability with a mild requirement. Various numerical simulations including the verification of accuracy, coarsening process and energy decay rate are presented to demonstrate the efficiency and the robustness of proposed schemes.

Key words: *Cahn-Hilliard equation, backward differentiation formula schemes, energy stability, Fourier collocation spectral method*

Introduction

The Cahn-Hilliard (CH) equation [1], which describes two-phase and multiphase problems involving fluid interfaces and the effect of surface tensions, is one of the most important fluid mechanics models in mathematical physics. For any $\phi \in H^1(\Omega)$, with $\Omega \subset R^2$, the Ginzburg-Landau energy functional of the CH model is given by:

$$E(\phi) = \int_{\Omega} \left(\frac{1}{4}\phi^4 - \frac{1}{2}\phi^2 + \frac{\varepsilon^2}{2}|\nabla\phi|^2 \right) \mathrm{d}x \tag{1}$$

in which $\Omega = (0, L_x) \times (0, L_y)$, the positive constant ε stands for the parameter of the interface width and ϕ represents the difference of the phase concentration. The CH equation can be viewed as the H^{-1} conserved gradient flow of the energy functional (1):

$$\phi_t = \Delta\mu, \text{ with } \mu := \delta_\phi E = \phi^3 - \phi - \varepsilon^2\Delta\phi \tag{2}$$

where a periodic boundary condition is imposed for both the phase field ϕ and the chemical potential μ. Owing to the gradient structure, the following energy dissipation:

* Corresponding author, e-mail: zhengkelong@swust.edu.cn

$$d_t E(t) = -\int_{\Omega} |\nabla \mu|^2 \, \mathrm{d}x \le 0 \tag{3}$$

holds. Furthermore, the equation is mass conservative $\int_{\Omega} \partial_t \phi \, \mathrm{d}x \le 0$, with the periodic boundary.

The CH equation is a fourth-order stiff non-linear PDE. To obtain accurate numerical solutions of such a problem, it is desirable to use high-order approximations in space and in time. There have extensive works to develop and analyze numerical schemes for the CH equation [2-4] and related models [5]. Among these results, the energy stability is an important issue since it plays an essential role for the long time numerical simulations. In particular, the convex splitting scheme should be addressed. The framework of convex splitting treats the convex part of the chemical potential implicitly and the concave explicitly and results in an unconditionally energy stable and uniquely solvable scheme. For example, see the finite element method [6], the mixed finite element method [7], and so forth.

The backward differentiation formula (BDF) is an implicit method for the numerical integration of ODE and especially used for the solution of stiff PDE. The BDF scheme treats the approximation every time at the time step t^{n+1} and requires less computational effort for the non-linear solver, due to the simpler form and stronger convexity properties of the non-linear term. For the CH equation, a second-order BDF mixed finite element scheme is presented by Yan *et al.* [8] and the similar idea also is used in [9]. The purpose of this paper is to construct and analyze a few second order in time semi-implicit Fourier collocation spectral schemes for CH equation by virtue of the BDF three-point stencil in the temporal approximation. An alternative Douglas-Dupont regularization term as $(-\Delta_N)^{\alpha}(\phi^{m+1} - \phi^m)$ is added, which can guarantee the energy stability, provided that the requirements of A are enforced for different values of the parameter α. In more details, we proposed three schemes, named as BDF-0 (corresponds to $\alpha = 0$), BDF-1 ($\alpha = 1$), and BDF-2 ($\alpha = 2$), respectively. On the other hand, the long time simulation results for the coarsening process indicate the requirement of the larger time step. Therefore, an extra artificial diffusion term is also introduced. The results show theoretically and numerically that the BDF-2 scheme can achieve the best stability performance.

Notations of Fourier collocation spectral approximations

Assume that $L_x = N_x h_x$, $L_y = N_y h_y$ for some mesh sizes h_x, $h_y > 0$ and some positive integers N_x and N_y. For simplicity of presentation, we use a square domain, *i.e.* $L_x = L_y = 1$, and a uniform mesh size $h_x = h_y = h$, $N_y = N_y = N$. We will assume that $N = 2K + 1$ is always odd. All the variables are evaluated at the regular numerical grid (x_i, y_j), with $x_i = ih$, $y_j = jh$, $0 \le i, j \le N$.

For a periodic function f over the given 2-D numerical grid, we define the grid function space:

$$G_n := \{f : Z^2 \to R \mid f \text{ is periodic}\}$$

Also, the zero-mean grid function subspace is denoted $\bar{G}_n := \{ f \in G_n \mid \langle f, 1 \rangle =: \bar{f} = 0 \}$. For $f \in G_n$, its discrete Fourier expansion is given by:

$$f_{(i,j)} = \sum_{l,m=-K}^{k} \hat{f}_{l,m} \exp[2\pi i(lx_i + my_j)] \tag{4}$$

Its approximations to first and second order partial derivatives are given by:

$$(\mathrm{D}_x f)_{i,j} = \sum_{l,m=-K}^{K} (2\pi i l)\, \hat{f}_{l,m} \exp[2\pi i(lx_i + my_j)]$$

$$(\mathrm{D}_x^2 f)_{i,j} = \sum_{l,m=-K}^{K} (-4\pi^2 l^2)\, \hat{f}_{l,m} \exp[2\pi i(lx_i + my_j)] \tag{5}$$

and the corresponding collocation spectral differentiations in the *y*-direction can be defined in the same way. In turn, the discrete Laplacian, gradient and divergence become:

$$\Delta_N f = (\mathrm{D}_x^2 + \mathrm{D}_y^2) f, \quad \nabla_N f = \begin{pmatrix} \mathrm{D}_x f \\ \mathrm{D}_y f \end{pmatrix}, \quad \nabla_N \begin{pmatrix} f_1 \\ f_2 \end{pmatrix} = \mathrm{D}_x f_1 + \mathrm{D}_y f_2$$

at the point-wise level. It is also straightforward to verify that : $\nabla_N \nabla_N f = \Delta_N f$.

We also introduce the discrete operator $(-\Delta_N)^{-\gamma}$. For a grid function f of (discrete) mean zero: $f \in \dot{G}_{\mathrm{n}}$, a discrete version of the operator $(-\Delta)^{-\gamma}$ may be defined:

$$(-\Delta_N)^{-\gamma} f_{i,j} := \sum_{l,m=-K,(l,m)\neq 0}^{K} [4\pi^2 (l^2 + m^2)]^{-\gamma}\, \hat{f}_{l,m} \exp[2\pi \mathrm{i}(lx_i + my_j)]$$

Detailed calculations show that the following summation-by-parts formulas are valid for any periodic grid functions $f, g \in G_{\mathrm{n}}$:

$$\langle f, \Delta_N g \rangle = \langle -\nabla_N f, \nabla_N g \rangle, \quad \langle f, \Delta_N^2 g \rangle = \langle \Delta_N f, \Delta_N g \rangle \tag{6}$$

Similarly, the following summation-by-parts formula is also available: for any $\gamma \geq 0$:

$$\langle f, (-\Delta_N)^{\gamma} g \rangle = \langle (-\Delta_N)^{\gamma/2} f, (-\Delta_N)^{\gamma/2} g \rangle \tag{7}$$

Since the CH eq. (2) is an H^{-1} gradient flow, we need a discrete version of the norm $\|\cdot\|_{H^{-1}}$ defined on G_{n}. Then, for any $f \in G_{\mathrm{n}}$, we define $\| f \|_{-1,N} := \| (-\Delta_N)^{-1/2} f \|_2$, and the following summation-by-parts formula may be derived:

$$\langle f, (-\Delta_N)^{-1} g \rangle = \langle (-\Delta_N)^{-1/2} f, (-\Delta_N)^{-1/2} g \rangle$$

Moreover, the spectral approximations to the l^2 inner product and norm are introduced:

$$\| f \|_2 = \sqrt{\langle f, f \rangle}, \text{ with } \langle f, g \rangle = h^2 \sum_{i,j=0}^{N-1} f_{i,j} g_{i,j}$$

The fully discrete BDF scheme and energy stability

In this section, we propose some BDF numerical schemes with Fourier collocation spectral approximation in space for CH eq. (2). In more details, a second order BDF discreti-

zation at t^{n+1} is used for the temporal discretization. Following the convex splitting idea, the non-linear term and the surface diffusion term are treated implicitly, and the concave diffusion term is handled by an explicit extrapolation formula. To ensure the energy stability of the numerical scheme, we also add a Douglas-Dupont regularization $As(-\Delta_N)^{\alpha}(\phi^{m+1} - \phi^m)$ and the values of A and α will be specified later. Furthermore, to understand the coarsening dynamics occurring on a very long time scale for small ϵ, an artificial diffusion term $B\Delta(\phi^{m+1} - 2\phi^m + \phi^{m-1})$ has to be imposed.

With the Fourier collocation spectral discretization in space, the second order accurate in time BDF type numerical scheme can be formulated as follows: for $m \geq 1$, given ϕ^m, $\phi^{m-1} \in G_n$, find $\phi^{m+1} \in G_n$ such that:

$$\frac{3\phi^{m+1} - 4\phi^m + \phi^{m-1}}{2s} = \Delta_N[(\phi^{m+1})^3 - (2\phi^m - \phi^{m-1}) - \epsilon^2\Delta_N\phi^{m+1}] -$$
$$-As(-\Delta_N)^{\alpha}(\phi^{m+1} - \phi^m) + B\Delta_N(\phi^{m+1} - 2\phi^m + \phi^{m-1}) \tag{8}$$

where $s = T/M$, A and B are the stability coefficients, $\alpha = 0,1$ or 2 means a different numerical scheme which requires a corresponding different energy-stability condition for A. We denote the scheme (8) with $\alpha = 0$ as BDF-0. Similarly, BDF-1 and BDF-2 are named for $\alpha = 1$ and $\alpha = 2$, respectively. For simplicity, on the initial step we assume $\phi^{-1} \equiv \phi^0$.

The second order BDF approximation (8) leads to a large region of absolute stability, in which an explicit Adams-Bashforth extrapolation formula is used to stabilize the concave term. The unconditional energy stability for the numerical scheme can be established and the uniquely solvability also can be straightforwardly obtained following a similar argument as in [8].

Before proceeding into further analysis, we make an observation. It is clear that the numerical solution of the fully discrete second order scheme (8) is mass-conserving at the discrete level if:

$$\overline{\phi^{m-1}} = \overline{\phi^m} = \phi_{av}, \text{ then } \overline{\phi^{m+1}} = \phi_{av}$$

We will assume that $|\phi_{av}| \leq 1$, as is standard.

We introduce a discrete energy, which is consistent with the continuous space energy (1), that is, for any periodic grid function $\phi \in G_n$, the discrete CH energy is defined as:

$$E_N(\phi) := \frac{1}{4}\|\phi\|_4^4 - \frac{1}{2}\|\phi\|_2^2 + \frac{\varepsilon^2}{2}\|\nabla_N\phi\|_2^2 \tag{9}$$

For the numerical scheme (8), we can not guarantee the energy E_N is non-increasing in time, but we can guarantee the dissipation of the modified version *via*:

$$\mathcal{E}_N(\phi,\psi) := E_N(\phi) + \frac{1}{4s}\|\phi - \psi\|_{-1,N}^2 + \frac{B+1}{2}\|\phi - \psi\|_2^2 \tag{10}$$

which is also consistent with the continuous case (1) as $s \to 0$ and $h \to 0$.

Theorem. For any $B \geq 0$ and given $\phi^{m-1}, \phi^m \in G_n$, the numerical schemes (8) are unconditionally energy stable under certain conditions for different values of α, *i.e.* for any positive integer $1 \leq m \leq M - 1$, the scheme (8) has the energy-decay property, with respect to the modified discrete energy:

$$\mathcal{E}_N(\phi^{m+1},\phi^m) \leq \mathcal{E}_N(\phi^m,\phi^{m-1}) \leq \mathcal{E}_N(\phi^0,\phi^{-1}) \leq C_0 \tag{11}$$

provided that the following condition holds: (1) $A \geq [1/(4\epsilon)]^4$ for BDF-0 scheme, (2) $A \geq 1/(2s)$ for BDF-1 scheme or (3) $A \geq 1/16$ for BDF-2 scheme.

Proof Taking a discrete inner product of (8) with $(-\Delta_N)^{-1}(\phi^{m+1} - \phi^m)$ yields:

$$\left\langle \frac{3\phi^{m+1} - 4\phi^m + \phi^{m-1}}{2s}, (-\Delta_N)^{-1}(\phi^{m+1} - \phi^m) \right\rangle =$$

$$= \left\langle \Delta_N[(\phi^{m+1})^3 - (2\phi^m - \phi^{m-1}) - \varepsilon^2 \Delta_N \phi^{m+1}], (-\Delta_N)^{-1}(\phi^{m+1} - \phi^m) \right\rangle -$$

$$- \left\langle As(-\Delta_N)^{\alpha}(\phi^{m+1} - \phi^m), (-\Delta_N)^{-1}(\phi^{m+1} - \phi^m) \right\rangle +$$

$$+ B\left\langle \Delta_N(\phi^{m+1} - 2\phi^m + \phi^{m-1}), (-\Delta_N)^{-1}(\phi^{m+1} - \phi^m) \right\rangle \tag{12}$$

The temporal term could be evaluated:

$$\left\langle \frac{3\phi^{m+1} - 4\phi^m + \phi^{m-1}}{2s}, (-\Delta_N)^{-1}(\phi^{m+1} - \phi^m) \right\rangle \geq$$

$$\geq \frac{1}{s}\left[\frac{3}{2}\| \phi^{m+1} - \phi^m \|^2_{-1,N} - \frac{1}{4}(\| \phi^{m+1} - \phi^m \|^2_{-1,N} + \| \phi^m - \phi^{m-1} \|^2_{-1,N})\right] =$$

$$= \frac{1}{s}\left[\frac{5}{4}(\| \phi^{m+1} - \phi^m \|^2_{-1,N}) - \frac{1}{4}\| \phi^m - \phi^{m-1} \|^2_{-1,N}\right] \tag{13}$$

For the non-linear term, the following estimate is valid:

$$-\left\langle \Delta_N(\phi^{m+1})^3, (-\Delta_N)^{-1}(\phi^{m+1} - \phi^m) \right\rangle = \left\langle (\phi^{m+1})^3, \phi^{m+1} - \phi^m \right\rangle \geq$$

$$\geq \| \phi^{m+1} \|^4_4 - \left(\frac{3}{4}\| \phi^{m+1} \|^4_4 + \frac{1}{4}\| \phi^m \|^4_4\right) = \frac{1}{4}\| \phi^{m+1} \|^4_4 - \frac{1}{4}\| \phi^m \|^4_4 \tag{14}$$

in which the Young inequality $ab \leq a^p/p + b^q/q, 1/p + 1/q = 1, (p = 4/3, q = 4)$ is applied.

For the surface diffusion term, we get:

$$\left\langle \Delta_N^2 \phi^{m+1}, (-\Delta_N)^{-1}(\phi^{m+1} - \phi^m) \right\rangle = \left\langle \nabla_N \phi^{m+1}, \nabla_N(\phi^{m+1} - \phi^m) \right\rangle =$$

$$= \frac{1}{2}(\| \nabla_N \phi^{m+1} \|^2_2 - \| \nabla_N \phi^m \|^2_2) + \frac{1}{2}\| \nabla_N(\phi^{m+1} - \phi^m) \|^2_2 \tag{15}$$

In turn, for the concave term and the artificial diffusion term, we get:

$$\left\langle \Delta_N(2\phi^m - \phi^{m-1}), (-\Delta_N)^{-1}(\phi^{m+1} - \phi^m) \right\rangle =$$

$$= -\left\langle \phi^m, \phi^{m+1} - \phi^m \right\rangle - \left\langle \phi^m - \phi^{m-1}, \phi^{m+1} - \phi^m \right\rangle \geq$$

$$\geq -\frac{1}{2}(\| \phi^{m+1} \|^2_2 - \| \phi^m \|^2_2) - \frac{1}{2}\| \phi^m - \phi^{m-1} \|^2_2 \tag{16}$$

and

$$-\left\langle \Delta_N(\phi^{m+1}-2\phi^m+\phi^{m-1}),(-\Delta_N)^{-1}(\phi^{m+1}-\phi^m)\right\rangle \geq \frac{1}{2}(\| \phi^{m+1}-\phi^m \|_2^2 - \| \phi^m-\phi^{m-1} \|_2^2)$$

Now, we consider the stabilizing term:

$$As\left\langle (-\Delta_N)^{\alpha}(\phi^{m+1}-\phi^m),(-\Delta_N)^{-1}(\phi^{m+1}-\phi^m)\right\rangle \tag{17}$$

for different values of α.

Case I: if $\alpha = 0$, it follows from (17) that:

$$As\left\langle (\phi^{m+1}-\phi^m),(-\Delta_N)^{-1}(\phi^{m+1}-\phi^m)\right\rangle = As\| \phi^{m+1}-\phi^m \|_{-1,N}^2 \tag{18}$$

Therefore, the combination of (13)-(16) and (18) yields that:

$$\mathcal{E}_N(\phi^{m+1},\phi^m)-\mathcal{E}_N(\phi^m,\phi^{m-1})-\frac{1}{2}\| \phi^{m+1}-\phi^m \|_2^2+\frac{1}{s}\| \phi^{m+1}-\phi^m \|_{-1,N}^2+$$

$$+\frac{\varepsilon^2}{2}\| \nabla_N(\phi^{m+1}-\phi^m) \|_2^2+As\| \phi^{m+1}-\phi^m \|_{-1,N}^2\leq 0 \tag{19}$$

Note that:

$$\frac{1}{s}\| \phi^{m+1}-\phi^m \|_{-1,N}^2+As\| \phi^{m+1}-\phi^m \|_{-1,N}^2+\frac{\varepsilon^2}{2}\| \nabla_N(\phi^{m+1}-\phi^m) \|_2^2\geq$$

$$\geq 2A^{1/2}\| \phi^{m+1}-\phi^m \|_{-1,N}^2+\frac{\varepsilon^2}{2}\| \nabla_N(\phi^{m+1}-\phi^m) \|_2^2\geq 2A^{1/4}\varepsilon\| \phi^{m+1}-\phi^m \|_2^2 \tag{20}$$

From eq. (20), we have:

$$\mathcal{E}_N(\phi^{m+1},\phi^m)-\mathcal{E}_N(\phi^m,\phi^{m-1})+\left(2A^{1/4}\varepsilon-\frac{1}{2}\right)\| \phi^{m+1}-\phi^m \|_2^2\leq 0 \tag{21}$$

which indicates $\mathcal{E}_N(\phi^{m+1},\phi^m)\leq \mathcal{E}_N(\phi^m,\phi^{m-1})$ provided that $A\geq (1/4\varepsilon)^4$.

Case II: if $\alpha = 1$, (17) becomes:

$$As\left\langle (-\Delta_N)(\phi^{m+1}-\phi^m),(-\Delta_N)^{-1}(\phi^{m+1}-\phi^m)\right\rangle = As\| \phi^{m+1}-\phi^m \|_2^2, \tag{22}$$

and eq. (13) can be revised as:

$$\mathcal{E}_N(\phi^{m+1},\phi^m)-\mathcal{E}_N(\phi^m,\phi^{m-1})+\left(As-\frac{1}{2}\right)\| \phi^{m+1}-\phi^m \|_2^2+$$

$$+\frac{1}{s}\| \phi^{m+1}-\phi^m \|_{-1,N}^2+\frac{\varepsilon^2}{2}\| \nabla_N(\phi^{m+1}-\phi^m) \|_2^2\leq 0 \tag{23}$$

Similarly, the following inequality is valid.,

$$\frac{1}{s}\| \phi^{m+1}-\phi^m \|_{-1,N}^2+\frac{\varepsilon^2}{2}\| \nabla_N(\phi^{m+1}-\phi^m) \|_2^2\geq \sqrt{2\frac{\varepsilon^2}{s}}\| \phi^{m+1}-\phi^m \|_2^2 \tag{24}$$

Accordingly, we have:

$$\mathcal{E}_N(\phi^{m+1},\phi^m)-\mathcal{E}_N(\phi^m,\phi^{m-1})+(\sqrt{2\frac{\varepsilon^2}{s}}+As-1/2)\,\|\,\phi^{m+1}-\phi^m\,\|_2^2\le 0 \tag{25}$$

Letting $(\sqrt{2\varepsilon^2/s}+As-1/2)\ge 0,$ we get $A\ge 1/(2s)-\sqrt{2\varepsilon^2/s^3}\ge 1/(2s).$ Therefore, in this case, if $A\ge 1/(2s),$ (11) also holds.

Case III: if $\alpha=2,$ (17) becomes:

$$As\left\langle(-\Delta_N)^2(\phi^{m+1}-\phi^m),(-\Delta_N)^{-1}(\phi^{m+1}-\phi^m)\right\rangle=As\,\|\,\nabla_N(\phi^{m+1}-\phi^m)\,\|_2^2 \tag{26}$$

and a similar result is obtained:

$$\mathcal{E}_N(\phi^{m+1},\phi^m)-\mathcal{E}_N(\phi^m,\phi^{m-1})-\frac{1}{2}\|\,\phi^{m+1}-\phi^m\,\|_2^2+\frac{1}{s}\|\,\phi^{m+1}-\phi^m\,\|_{-1,N}^2+$$

$$+\frac{\varepsilon^2}{2}\|\,\nabla_N(\phi^{m+1}-\phi^m)\,\|_2^2+As\,\|\,\nabla_N(\phi^{m+1}-\phi^m)\,\|_2^2\ge$$

$$\ge\mathcal{E}_N(\phi^{m+1},\phi^m)-\mathcal{E}_N(\phi^m,\phi^{m-1})+\left(2\sqrt{(As+\varepsilon^2/2)/s}-1/2\right)\|\,\phi^{m+1}-\phi^m\,\|_2^2$$

Clearly, if the coefficient $(2\sqrt{(As+\varepsilon^2/2)/s}-1/2)\ge 0,$ that is, $A\ge 1/16-\varepsilon^2/(2s)$ or the mild low bound $A\ge 1/16,$, we also get (11). This completes the proof.

Accuracy test

In this subsection we perform a numerical accuracy check for the fully discrete second order scheme (8). The 2-D computational domain is set to be $\Omega=(0,1)^2,$ and the exact profile for the phase variable is given by

$$\Phi(x,y,t)=\sin(2\pi x)\cos(2\pi y)\cos(t) \tag{27}$$

To make Φ satisfy the original PDE (2), we have to add an artificial, time-dependent forcing term. For exploring the temporal accuracy, we compute solutions with grid sizes N = 16-256, and the errors are reported at the final time T = 1. The time step is determined by the linear refinement path: s = 0.5h, where h is the spatial grid size. We choose parameters: $\varepsilon^2=0.01, A=1, B=1.$ Table 1 shows the discrete $\|\cdot\|_2$ norms and the convergence orders of the errors between the numerical and exact solutions for the scheme BDF-0, BDF-1, and BDF-2, respectively.

Table 1. The $\|\cdot\|_2$ errors and the orders with ε^2 = 0.01, A = 1, B = 1

Scheme	BDF-0		BDF-1		BDF-2	
N	$\|\cdot\|_2$	order	$\|\cdot\|_2$	order	$\|\cdot\|_2$	order
16	$1.7489\cdot10^{-3}$	–	$2.8452\cdot10^{-3}$	–	$5.3985\cdot10^{-2}$	–
32	$4.4570\cdot10^{-4}$	1.972	$7.4494\cdot10^{-4}$	1.933	$1.9654\cdot10^{-2}$	1.457
64	$1.1175\cdot10^{-4}$	1.995	$1.8889\cdot10^{-4}$	1.979	$5.8520\cdot10^{-3}$	1.747
128	$2.7893\cdot10^{-5}$	2.002	$4.7361\cdot10^{-5}$	1.995	$1.5538\cdot10^{-3}$	1.913
256	$6.9625\cdot10^{-6}$	2.002	$1.1843\cdot10^{-5}$	1.999	$3.9521\cdot10^{-4}$	1.975

Coarsening processes and energy dissipation in time

A numerical simulation result of a physics example is presented in this subsection. In particular, the long time evolution scaling law for certain physical quantities, such as the energy, has caused a great deal of scientific interests, with the assumption that the interface width is in a much smaller scale than the domain size, *i.e.*, $\varepsilon \ll \min\{L_x, L_y\}$, with $\Omega = (0, L_x) \times (0, L_y)$. A formal analysis has indicated a lower decay bound as $t^{-1/3}$ for the energy dissipation law, with the lower bound typically observed for the averaged values of the energy quantity.

We compare the numerical simulation result with the predicted coarsening rate, using the proposed second order scheme BDF-2 in (8) for the CH flow (2). The diffusion parameter is taken to be $\varepsilon^2 = 0.005$. For the domain we take $L_x = L_y = L = 12.8$ and $h = L/N$, where h is the uniform spatial step size. For such a value of ε, our numerical experiment has shown that $N = 256$ is sufficient to resolve the small structures in the solution.

For the temporal step size s, we use increasing values of s in the time evolution. In more detail, $s = 0.004$ on the time interval [0,100], $s = 0.01$ on the time interval [100,1000], and $s = 0.02$ on the time interval [1000, 2000]. Whenever a new time step size is applied, we initiate the two-step numerical scheme by taking $\phi^{-1} = \phi^0$, with the initial data ϕ^0 given by the final time output of the last time period. Figures 1 and 2 present time snapshots of the phase variable ϕ with $\varepsilon^2 = 0.005$. A significant coarsening process is clearly observed in the system. At early times many small structures are present. At the final time $t = 2000$, a single interface structure emerges, and further coarsening is not possible.

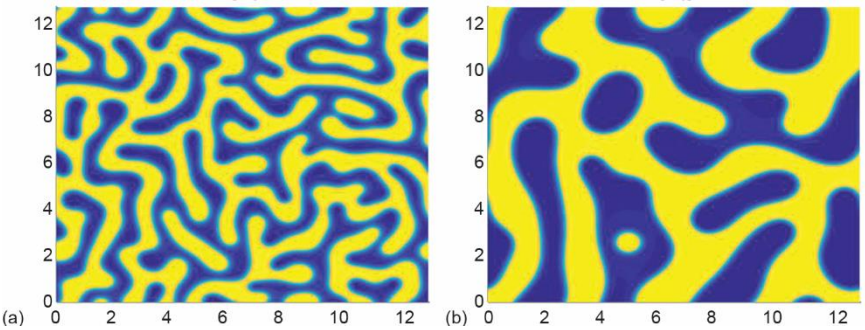

Figure 1. Snapshots of the phase variable at (a) $t = 1$ and (b) $t = 10$
(*for color image see journal web site*)

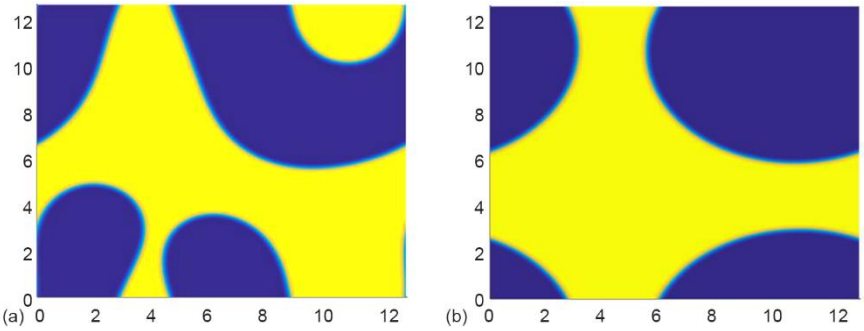

Figure 2. Snapshots of the phase variable at (a) $t = 200$ and (b) $t = 2000$
(*for color image see journal web site*)

The long time characteristics of the solution, especially the energy decay rate, are of interest to material scientists. Recall that, at the space-discrete level, the energy, E_N is defined *via* (9). To facilitate the energy scaling analysis, we add a constant $|\Omega|/4$ to the energy introduced by (1):

$$\tilde{E}(\phi) = \int_{\Omega} \left(\frac{1}{4}\phi^4 - \frac{1}{2}\phi^2 + \frac{1}{4} + \frac{\varepsilon^2}{2} |\nabla \phi|^2 \right) \mathrm{d}x = E(\phi) + \frac{1}{4} |\Omega| \tag{28}$$

As a result, this energy is always non-negative. Figure 3 presents the log-log plot for the energy *vs.* time, with the given physical parameter $\varepsilon^2 = 0.005$ (the line 1 represents the energy plot obtained by the simulations, while the line 2 is obtained by least squares approximations to the energy data only up to about time $t = 200$). The detailed scaling *exponent* is obtained using least squares fits of the computed data up to time. A clear observation of the at^b scaling law can be made, with $a = 10.7394$, $b = -0.3608$. In other words, an almost perfect $t^{-1/3}$ energy dissipation law is confirmed by our numerical simulation.

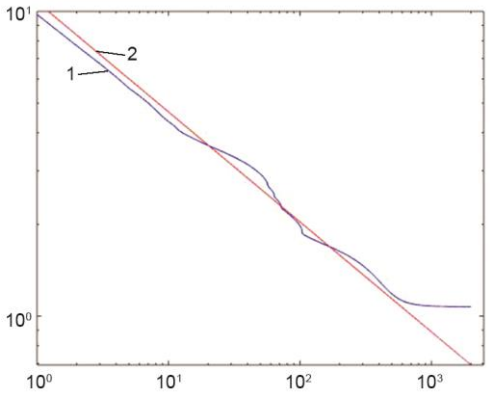

Figure 3. Log-log plot of the temporal evolution the energy $t = 200$ for $\varepsilon^2 = 0.005$

Conclusion

In this paper, we have presented some energy-stable second order in time BDF numerical schemes for the CH equation with the Fourier collocation spectral approximation in space.

The energy stability properties of three proposed BDF schemes which are designed for large-system and long-time simulations are analyzed. Numerical experiments also have shown the second order accuracy and long time coasening results.

Nomenclature

A, B – adjustable parameters
D_x – first order partial derivative
D_x^2 – second order partial derivative
E – energy functional
ε_N – modified energy functional
$f_{l,m}$ – Fourier coefficient
h – spatial step size
s – temporal step size
t – time
G_n – grid function space
Δ – Laplacian operator
∇ – divergence operator
Δ_N – discrete Laplacian operator
∇_N – discrete divergence operator

Greek symbols

ϕ – phase variable
ϕ^m – numerical solution at t^m
δ_ϕ – variation in ϕ
μ – chemical potential
ε – interface width
Ω – domain
$\overline{\phi^m}$ – mean value of numerical solutions

Acronyms

BDF – backward differentiation formula
CH – Cahn-Hilliard

References

[1] Cahn, J. W., Hilliard, J. E., Free Energy of a Nonuniform System, I. Interfacial Free Energy, *Journal of Chemical Physics,* 28 (1958), 2, pp. 258-267

[2] Chen, F., Shen, J., Efficient Energy Stable Schemes with Spectral Discretization in Space for Anisotropic Cahn-Hilliard systems, *Communications in Computational Physics*, *13* (2013), 5, pp. 1189-1208
[3] Cheng, K., *et al.*, A Second-Order, Weakly Energy-Stable Pseudo-Spectral Scheme for the Cahn-Hilliard Equation and Its Solution by the Homogeneous Linear Iteration Method, *Journal of Scientific Computing*, *69* (2016), 3, pp. 1083-1114
[4] Cheng, K., *et al.*, An Energy Stable Fourth Order Finite Difference Scheme for the Cahn-Hilliard Equation, *Journal of Computational and Applied and Mathematics*, *362* (2019), Dec., pp. 574-595
[5] Cheng, K., *et al.*, A Third Order Exponential Time Differencing Numerical Scheme for No-Slope-Selection Epitaxial Thin Film Model with Energy Stability, *Journal of Scientific Computing*, *81* (2019), 1, pp. 154-185
[6] Furihata, D., A Stable and Conservative Finite Difference Scheme for the Cahn-Hilliard Equation, *Numerische Mathematik*, *87* (2001), 4, pp. 675-699
[7] Diegel, A., *et al.*, Stability and Convergence of a Second Order Mixed Finite Element Method for the Cahn-Hilliard Equation, *IMA Journal of Numerical Analysis*, *36* (2016), 4, pp. 1867-1897
[8] Yan, Y., *et al.*, A Second-Order Energy Stable BDF Numerical Scheme for the Cahn-Hilliard Equation, *Communications in Computational Physics*, *23* (2018), 2, pp. 572-602
[9] Li, D., Qiao, Z., On Second Order Semi-Implicit Fourier Spectral Methods for 2-D Cahn-Hilliard Equations, *Journal of Scientific Computing*, *70* (2017), 1, pp. 301-341

Paper submitted: June 1, 2021
Paper revised: July 20, 2021
Paper accepted: July 29, 2021